Photonic-crystal fiber-based pressure sensor for dual environment monitoring

Jonas H. Osório,[1,*,†] Juliano G. Hayashi,[1,†] Yovanny A. V. Espinel,[1] Marcos A. R. Franco,[2] Miguel V. Andrés,[3] and Cristiano M. B. Cordeiro[1]

[1]Instituto de Física "Gleb Wataghin", UNICAMP, Campinas, SP, Brazil

[2]Instituto de Estudos Avançados, Comando Tecnológico da Aeronáutica, CTA, São José dos Campos, SP, Brazil

[3]Departamento de Física Aplicada-ICMUV, Universitat de Valencia, Valencia, Spain

*Corresponding author: jhosorio@ifi.unicamp.br

Received 7 April 2014; accepted 22 April 2014;
posted 7 May 2014 (Doc. ID 208745); published 4 June 2014

In this paper the development of a side-hole photonic-crystal fiber (SH-PCF) pressure sensor for dual environment monitoring is reported. SH-PCF properties (phase and group birefringence, sensitivity to pressure variations) are measured and compared to simulated data. In order to probe two environments, two sections of the SH-PCF with different lengths are spliced and set in a Solc filter-like configuration. This setup allows obtaining the individual responses of the first and second fiber independently, which is useful for a space-multiplexed measurement. As the employed fiber is sensitive to pressure variations, we report the use of this configuration for dual environment pressure sensing.

OCIS codes: (060.2310) Fiber optics; (060.2370) Fiber optics sensors; (060.5295) Photonic crystal fibers; (120.5475) Pressure measurement.

http://dx.doi.org/10.1364/AO.53.003668

1. Introduction

Photonic crystal fibers (PCF) are an excellent platform for sensing applications due to their inherent design versatility [1]. By adequately choosing the microstructure, fiber characteristics can be tailored in order to optimize the physical properties of interest. This versatility permits the development of a great variety of PCF-based sensors for the monitoring of different physical quantities (e.g., hydrostatic pressure [2], strain [3], and curvature [4]).

The properties of PCFs can be chosen in such a way that their optical response is dependent on hydrostatic pressure variations. This dependence is mediated by the geometrical and photoelastic effects and is highly dependent on PCF microstructure geometry [5]. Birefringent PCFs are often used to build up hydrostatic pressure sensors, as reported in previous papers [2,5,6,7]. In these papers authors perform pressure sensing measurements by two means: either exploring the phase birefringence dependence on pressure variations or studying the spectral behavior of a fiber subjected to different pressure conditions in an interferometric configuration.

In the first case, the physical quantity to be analyzed is the phase birefringence derivative with respect to pressure ($\partial B/\partial P$) and the measurement is performed by using a laser as the light source and a photodetector for taking information about the transmitted power. $\partial B/\partial P$ value depends on the wavelength (λ), the length of the fiber submitted to external pressure (L_p) and on the pressure T needed to rotate the fiber output light polarization π rad (one polarization cycle). This dependence is expressed by Eq. (1) [2],

1559-128X/14/173668-05$15.00/0

$$\frac{\partial B}{\partial P} = \frac{\lambda}{TL_p}. \quad (1)$$

The second type of measurement is based on the employment of a broadband light source and on the measurement of the spectral response of an interferometric configuration. This response is characterized by the existence of interferometric fringes whose spectral position is dependent on the pressure applied on the fiber, i.e., its spectral position shifts as the pressure is varied. In order to characterize this dependence, a sensitivity coefficient C_S is defined and its value can be accounted by Eq. (2) [6],

$$\frac{\Delta\lambda}{\Delta P} \equiv C_S \approx \frac{\lambda}{G}\frac{\partial B}{\partial P}, \quad (2)$$

where λ is the central wavelength of a local minimum in the spectra (destructive interference), $\Delta\lambda$ is the central wavelength shift caused by the application of external hydrostatic pressure, ΔP is the pressure variation, G is the group modal birefringence, and $\partial B/\partial P$ is the phase birefringence derivative with respect to pressure, as described before.

In this paper, we theoretically and experimentally studied the sensitivity of a side-hole PCF [(SH-PCF), a fiber with longitudinal holes beside the microstructured region [8]] to hydrostatic pressure variations and employed the same in a dual environment pressure sensing measurement. We focused on studying fiber properties and on obtaining the dual environment sensor. It is not our goal to report record pressure sensitivity values.

In order to build the sensor, we make use of a simple technique developed in our group at UNICAMP, which employs two birefringent fibers set in an in-series configuration. This technique, reported in [9], employs an input and an output polarizer whose angles are chosen in such a manner that the first or second fiber-individual responses can be independently obtained. By separately measuring the first and second fiber responses, we demonstrate the performance of a hydrostatic pressure sensor with two probing regions for dual environment monitoring.

2. Fiber Characterization

A side-hole SH-PCF [8,10] was chosen to act as the platform for the hydrostatic pressure sensing experiment due to its high sensitivity to pressure variations. Fiber cross-section is shown in Fig. 1(a). The inset presents an image of the microstructured region. Hole diameter ($d = 1.7$ μm) and separation ($\Lambda = 2.8$ μm) are also represented.

The experimental setup for performing the initial characterization measurements is represented in Fig. 1(b). The SH-PCF was previously spliced to standard single mode fibers and placed into a pressure chamber. The light source is polarized by the first polarizer (P_1) and launched into the SH-PCF in such a manner that both orthogonal modes of the birefringent fiber are excited. The output polarizer (P_2)

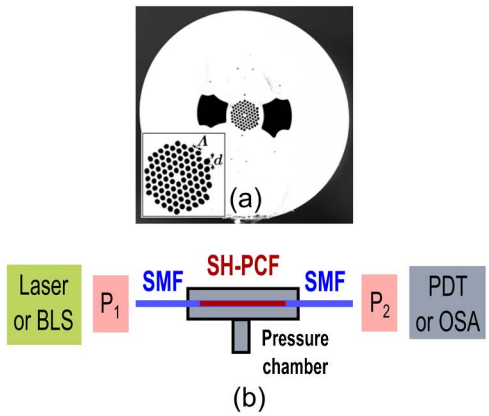

Fig. 1. (a) Cross-section of the SH-PCF used in the experiments. Inset exposes the microstructured region. Hole diameter ($d = 1.7$ μm) and separation ($\Lambda = 2.8$ μm) are shown. (b) Experimental setup for SH-PCF pressure sensitivity characterization. BLS, broadband light source; P_1 and P_2, polarizers; SMF, standard single mode fiber; SH-PCF: side-hole photonic-crystal fiber; PDT, photodetector; OSA, optical spectrum analyzer.

allows the light from the orthogonal modes to interfere and the optical response is measured by a photo-detector (PDT) or an optical spectrum analyzer (OSA).

In order to measure $\partial B/\partial P$, one uses the setup represented in Fig. 1(b) with a laser at 633 or 1550 nm as the light source and a photodetector connected to an oscilloscope as the measurement system. Due to the orthogonal mode's different phase velocities (effective refractive indices are different), they reach the end of the fiber with a phase difference ($\Delta\varphi$), which is dependent on phase birefringence (B), fiber length (L), and wavelength (λ) of the light source as shown in Eq. (3),

$$\Delta\varphi = \frac{2\pi BL}{\lambda}. \quad (3)$$

For a fixed fiber length, phase difference $\Delta\varphi$ defines the output light polarization, which can be linear, circular—if $\Delta\varphi = \pi n$ or $\Delta\varphi = \pi(n + 1/2)$, respectively ($n$ is an integer)—or elliptical. When external pressure is applied on an SH-PCF, the anisotropic stress propagation in the microstructure changes the effective refractive index of both propagation axes of the fiber differently. Consequently, there is a variation in B, which generates a change in $\Delta\varphi$. Thus, the polarization state of the light that leaves the fiber is altered.

Figure 2(a) shows the optical response at 633 nm when 103 cm of SH-PCF is submitted to a pressure variation of 0.69 MPa (approximately 6.9 bar) during 1.7 s. The voltage signal from the photodetector (measured in an oscilloscope) oscillates as the pressure varies in time. The maximum and minimum occur when the output fiber light aligns with the passing and blocking polarizer axes, respectively. A complete signal oscillation (i.e., a polarization cycle, which corresponds to the interval between two

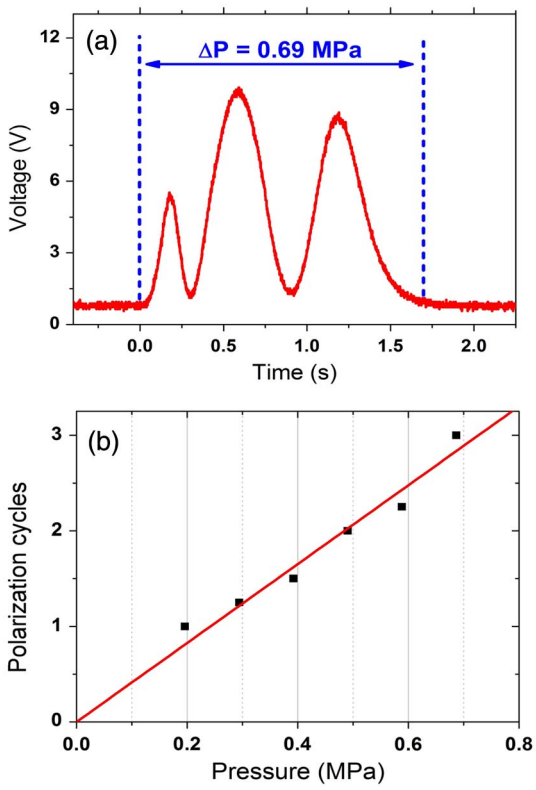

Fig. 2. Voltage signal from photodetector, which is related to the transmitted power, measured as the pressure was varied from 0.69 MPa to zero. (b) Polarization cycle plot as a function of the pressure applied on the fiber. Measurements taken at $\lambda = 663$ nm.

minima or maxima points) is related to a variation of π rad in the phase difference between axes of the light that arises from the fiber end. Figure 2(b) shows the polarization cycles plot of the fiber output as a function of the applied pressure at 633 nm.

Therefore, by experimentally obtaining the pressure T from the linear fit of the polarization cycles versus pressure (T is the inverse of the slope), it is possible to determine an experimental value for $\partial B/\partial P$. Experimentally obtained values for $\partial B/\partial P$ are $(2.6 \pm 0.1) \times 10^{-6}$ MPa^{-1} for $\lambda = 663$ nm and $(2.70 \pm 0.06) \times 10^{-6}$ MPa^{-1} for $\lambda = 1550$ nm. The value for $\partial B/\partial P$ obtained herein is comparable to the one reported in [5] for PM-1550-01 fiber: 2.32×10^{-6} MPa^{-1}. Our fiber $\partial B/\partial P$ value is smaller than the one found in [11] and [12], which theoretically calculated a value of 9.05×10^{-6} MPa^{-1} and 43.89×10^{-6} MPa^{-1} for other specially designed PCFs. Martynkien *et al.* [13] and Anuszkienwicz *et al.* [14] could experimentally verify even higher values for $\partial B/\partial P - 1.06 \times 10^{-5}$ MPa^{-1} and 2.70×10^{-5} MPa^{-1}.

For taking spectral measurements, one employs the setup schematized in Fig. 1(b). A supercontinuum generated by a PCF fiber is used as the light source and the measurement system is an OSA. Again, input polarization must be such that both orthogonal modes of the birefringent fiber are exited. After traveling along the fiber, the modes are recombined and the transmitted spectrum is measured by the OSA. A typical spectrum is shown in Fig. 3(a). Curvatures in standard fiber sections are minimal. It avoids degrading the polarization state of the light to be launched in the SH-PCF.

The spectrum presented in Fig. 3(a) allows calculating fiber group birefringence (G) by Eq. (4), where S is the wavelength difference between two consecutive dips in the spectrum and L is the length of the fiber [7]. Phase birefringence (B) can be calculated by Eq. (5), where γ is a fitting parameter related to the empirical relation expressed by Eq. (6) and obtained by a self-consistent method (A is another fitting constant) [15]. Figures 3(b) and 3(c) show the experimental results (points) for group and phase birefringence versus wavelength:

$$G(\lambda) = \frac{\lambda^2}{SL}. \tag{4}$$

$$B(\lambda) = \frac{\lambda}{2L}\left[\left(1 + \frac{S}{\lambda}\right)^{\gamma-1} - 1\right]^{-1} \tag{5}$$

$$B(\lambda) = A\lambda^{\gamma}. \tag{6}$$

To experimentally account for C_S [Eq. (2)], spectra are taken for situations in which different pressure values were applied on the fiber. A particular fringe is chosen and its wavelength shift is divided by the pressure variation. Experimentally measured C_S values are presented in Fig. 3(d). Due to the decrease (in modulus) of group birefringence, as expected from Eq. (2), C_S is higher for lower wavelengths. Theoretical values for B, G, and C_S were also calculated by employing a commercial finite-element method based software. Lines in Figs. 3(b)–3(d) presents simulated data for G, B, and C_S as a function of λ. Note that B and G have opposite sign for this fiber.

Moreover, Fig. 3(d) exposes a simulation for a commercial PCF usually employed in pressure sensing measurements (PM-1550-01 by NKT Photonics). SH-PCF proposed in this paper has a higher sensitivity coefficient than the commercial PCF. At $\lambda = 1550$ nm, for instance, the sensitivity coefficient for the SH-PCF is about 2.8 times higher than the one for the commercial PCF. We calculated the C_S value for the fiber reported in [11] and found it is 1.34-fold higher than the one of the fiber reported herein (at $\lambda = 1550$ nm). Anuszkienwicz *et al.* [14], in turn, by using a different technique (rocking filter inscribed in a PCF), could experimentally demonstrate an extremely high sensitivity value −177 nm/MPa.

3. Dual Environment Hydrostatic Pressure Sensing

After characterizing the SH-PCF, the fiber was used to build up an all-fiber sensor able to probe two different environments. To do this, one employs the technique recently reported in [9] where two birefringent

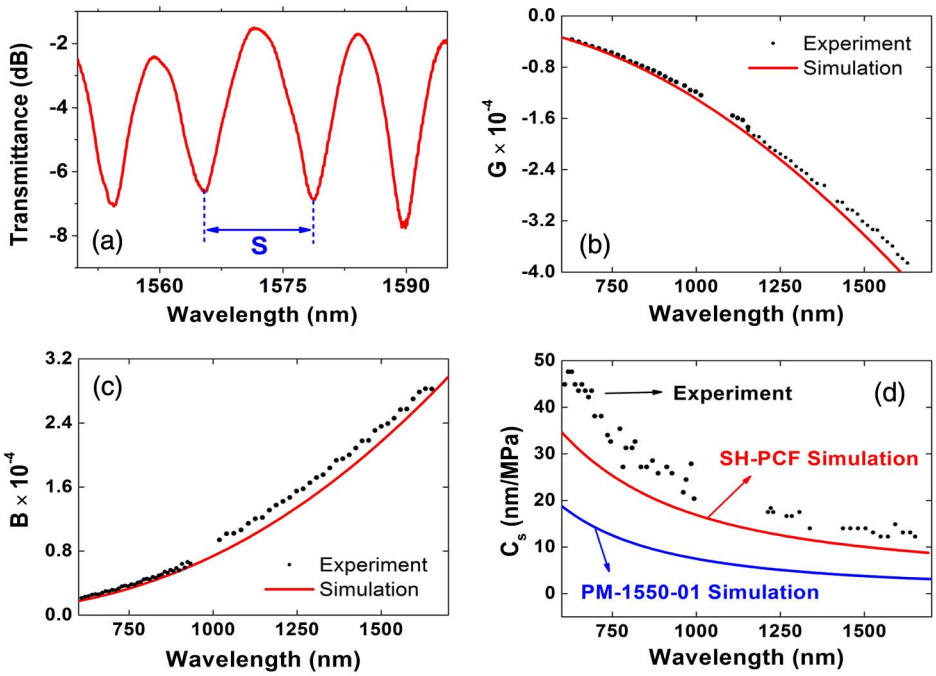

Fig. 3. (a) Typical spectrum for the transmittance as a function of the wavelength. Experimental and simulation results for (b) group birefringence, (c) phase birefringence, and (d) sensitivity coefficient C_s as a function of the wavelength.

fibers are spliced in such a way that their principal axes are rotated in relation to each other and placed in an experimental setup as schematized in Fig. 4.

Although fibers are spliced, it is possible to obtain single fiber responses by conveniently adjusting the input and output polarizers, i.e., one can measure the first or the second fiber responses separately by simply tuning the polarizer's angles. As reported in [9], for obtaining the first fiber response, the second polarizer must be aligned to one of the principal axes of the second fiber. Similarly, the condition for obtaining the second fiber response is launching light in the system with the input polarization along one of the principal axes of the first fiber.

In the experiment reported herein, two sections of the SH-PCF [with total lengths $L_1 = (22.5 \pm 0.02)$ cm and $L_2 = (58.5 \pm 0.02)$ cm] were spliced and put into two different pressure chambers (Fig. 4). After the first fiber response was obtained [Fig. 5(a) top], this fiber was subjected to different pressure conditions and spectra were recorded for every situation. Analogously, for the case in which the second fiber response was attained [Fig. 5(a) bottom], spectra were taken for different hydrostatic pressure values applied on the fiber. Figure 5(b) shows the wavelength shift of a particular dip as a function of the pressure applied on the fiber for the two situations just described. C_S values of (1.69 ± 0.04) nm/MPa and (2.22 ± 0.04) nm/MPa were obtained for the first and second fiber, respectively. This difference is justified by the fact that different fractions of the lengths of the fibers were pressurized (pressurized lengths: $L_{p1} = 2$ cm and $L_{p2} = 8$ cm). The predicted value for the relation between the C_s values to be measured (R) is given by Eq. (7). This equation follows from the development reported in [9] for the case in which the pressurized lengths of the fibers are different:

$$R \equiv \frac{C_{S1}}{C_{S2}} = \frac{L_{p1}}{L_{p2}} \frac{L_2}{L_1}. \tag{7}$$

According to Eq. (7), the predicted value for $R_{\text{predicted}}$ is (0.65 ± 0.08). Experimental values from Fig. 5(b) provide $R_{\text{experimental}} = (0.76 \pm 0.03)$. Thus, one can observe that the predicted and experimentally verified values for R are consistent.

Using the setup schematized in Fig. 4, for the situations in which the first and second fibers responses were obtained separately, $\partial B/\partial P$ values at $\lambda = 1550$ nm were measured in the same way that it was measured using the single-fiber configuration (by substituting the broadband light source by a one that is a laser). $\partial B/\partial P$ values obtained were $(2.5 \pm 0.2) \times 10^{-6}$ MPa^{-1} for the first fiber and $(2.9 \pm 0.3) \times 10^{-6}$ MPa^{-1} for the second one. The results are consistent with the one obtained in the

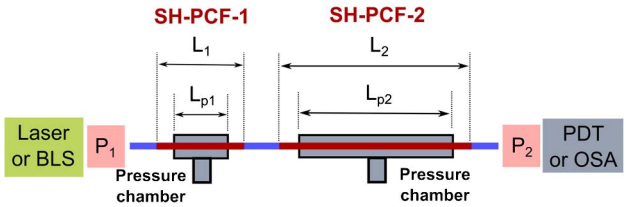

Fig. 4. Schematic diagram for the experimental setup for dual environment monitoring.

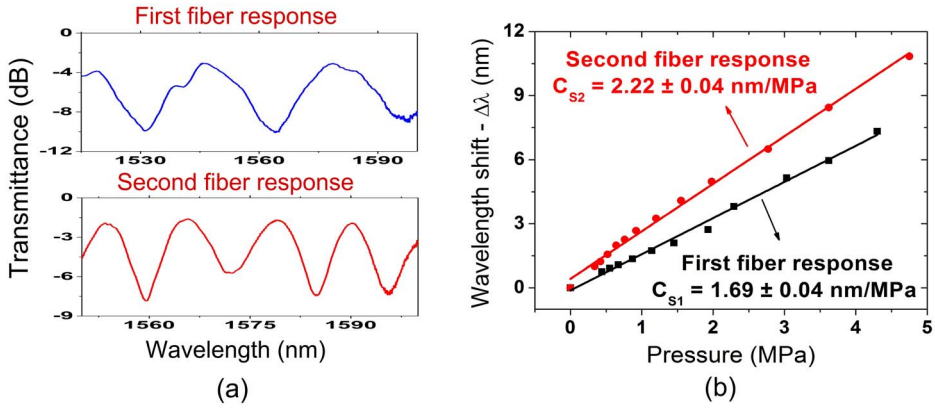

Fig. 5. (a) First and second fibers spectral response as the applied pressure is varied. (b) Wavelength shift as a function of the applied pressure on the fiber.

single-fiber configuration, $(2.70 \pm 0.06) \times 10^{-6}\,\mathrm{MPa}^{-1}$, as expected.

4. Conclusions

In this paper, the development of a pressure sensor with two sensitive regions for dual environment monitoring was presented. To do this, two sections of a SH-PCF were spliced in a series configuration and placed in a setup where input and output polarizers angles could be tuned in order to obtain separate fiber responses.

First, the fiber was characterized. Phase and group birefringence and the sensitivity parameter C_S were measured and compared to simulated values showing good agreement. Also, pressure sensitivity of the SH-PCF was compared to the one presented by the commercial fiber PM-1550-01 (NKT Photonics), usually employed in pressure measurements. SH-PCF sensitivity was found to be about 2.8-fold the PM-1550-01 respective value.

Finally, the dual environment pressure-sensor performance was demonstrated. The proposed configuration allows performing independent pressure measurements in two disconnected environments. Hence, the sensor was shown to have two sensing regions, which can be placed in the environments of interest for pressure variations probing.

Authors thank FINEP (project 01.12.0393/2012-8) and CNPq and for financial support.

†These authors contributed equally for the development of the research project.

References

1. P. Russel, "Photonic crystal fibers," Science **299**, 358–362 (2003).
2. G. Statkiewicz, T. Martynkien, and W. Urbanczyk, "Measurements of modal birefringence and polarimetric sensitivity of the birefringent holey fiber to hydrostatic pressure and strain," Opt. Commun. **241**, 339–348 (2004).
3. X. Dong, H. Y. Tam, and P. Shum, "Temperature-insensitive strain sensor with polarization-maintaining photonic crystal fiber based Sagnac interferometer," Appl. Phys. Lett. **90**, 151113 (2007).
4. H. Martins, M. B. Marques, P. Jorge, C. M. B. Cordeiro, and O. Frazão, "Intensity curvature sensor based on photonic crystal fiber with three coupled cores," Opt. Commun. **285**, 5128–5131 (2012).
5. M. Szpulak, T. Martynkien, and W. Urbanczyk, "Effects of hydrostatic pressure on phase and group modal birefringence in microstructurated holey fibers," Appl. Opt. **43**, 4739–4744 (2004).
6. F. C. Fávero, S. M. M. Quintero, C. Martelli, A. M. B. Braga, V. V. Silva, I. C. S. Carvalho, R. W. A. Llerena, and L. C. G. Valente, "Hydrostatic pressure sensing with high birefringence photonic crystal fibers," Sensors **10**, 9698–9711 (2010).
7. T. Nasilowski, T. Martynkien, G. Statkiewicz, M. Szpulak, J. Olszewski, G. Golojuch, W. Urbanczyk, J. Wojcik, P. Mergo, M. Makara, F. Berghmans, and H. Thienpont, "Temperature and pressure sensitivities of the highly birefringent photonic crystal fiber with core asymmetry," Appl. Phys. B **81**, 325–331 (2005).
8. H. M. Xie, P. Dabkiewicz, R. Ulrich, and K. Okamoto, "Side-hole fiber for fiber-optic pressure sensing," Opt. Lett. **11**, 333–335 (1986).
9. J. H. Osório and C. M. B. Cordeiro, "Optical sensor based on two in-series birefringent optical fibers," Appl. Opt. **52**, 4915–4921 (2013).
10. G. Chesini, V. A. Serrão, M. A. R. Franco, and C. M. B. Cordeiro, "Analysis and optimization of an all-fiber device based on photonic crystal fiber with integrated electrodes," Opt. Express **18**, 2842–2848 (2010).
11. M. Szpulak, T. Martynkien, and W. Urbanczyk, "Highly birefringent photonic crystal fibre with enhanced sensitivity to hydrostatic pressure," in *Proceedings of 2006 8th International Conference on Transparent Optical Networks and 5th Conference on Photonic Crystals* (IEEE, 2006) Vol. **4**, pp. 174–177.
12. C. M. Jewart, S. M. Quintero, A. M. B. Braga, and K. P. Chen, "Design of a highly birefringent microstructured photonic crystal fiber for pressure monitoring," Opt. Express **18**, 25657–25664 (2010).
13. T. Martynkien, G. Statkiewicz-Barabach, J. Olszewski, J. Wojcik, P. Mergo, T. Geernaert, C. Sonnenfeld, A. Anuszkiewicz, M. K. Szczurowski, K. Tarnowski, M. Makara, K. Skorupski, J. Klimek, K. Poturaj, W. Urbanczyk, T. Nasilowski, F. Berghmans, and H. Thienpont, "Highly birefringent microstructures fibers with enhanced sensitivity to hydrostatic pressure," Opt. Express **18**, 15113–15121 (2010).
14. A. Anuszkienwicz, G. Statkiewicz-Barabach, T. Borsukowski, J. Olszewski, T. Martynkien, W. Urbanczyk, P. Mergo, M. Makara, K. Poturaj, T. Geernaert, F. Berghmans, and H. Thienpont, "Sensing characteristics of the rocking filters in microstructured fibers optimized for hydrostatic pressure measurements," Opt. Express **20**, 23320–23330(2012).
15. K. Suzuki, H. Kubota, S. Kawanishi, M. Tanaka, and M. Fujta, "Optical properties of a low-loss polarization-maintaining photonic crystal fiber," Opt. Express **9**, 676–680 (2001).